

Raman response function for silica fibers

Q. Lin and Govind P. Agrawal

Institute of Optics, University of Rochester, Rochester, New York 14627

Received June 22, 2006; accepted July 31, 2006;

posted August 15, 2006 (Doc. ID 72217); published October 11, 2006

The commonly used Lorentzian form of the Raman response function for studying propagation of ultrashort pulses in silica fibers does not properly account for the shoulder in the Raman gain spectrum originating from the Boson peak. We propose a more accurate form of this response function and show that its predictions for the Raman-induced frequency shift should be in better agreement with experiments. © 2006 Optical Society of America

OCIS codes: 060.5530, 060.7140, 190.5650, 190.4370.

The nonlinear effects in optical fibers affect the propagation of ultrashort pulses considerably and lead to a variety of interesting optical phenomena, such as Raman-induced frequency shift (RIFS), soliton fission, and supercontinuum generation.¹ The Raman effect is known to impact ultrashort pulses, and its inclusion is essential in any theoretical modeling. Indeed, numerous efforts have been made to characterize the nonlinear properties of silica glass and fibers^{2–3} and to model the associated nonlinear response.^{9–11} In general, it has the form $R(\tau) = (1-f_R)\delta(\tau) + f_R h_R(\tau)$, where the two terms account for the instantaneous electronic and retarded molecular responses, respectively.¹ The Raman response function $h_R(\tau)$ exhibits complicated dynamics⁹ because of the amorphous nature of silica glass.^{2,3}

Although the Raman response can be modeled fairly accurately by a superposition of 13 complicated functions,¹¹ such a model is often impractical owing to its complexity. At the other extreme, the Raman response is approximated by damping oscillations associated with a single vibrational mode,¹⁰ resulting in a Lorentzian-shaped gain spectrum (dashed curve in Fig. 1). This model uses three parameters to provide the correct location and peak value of the dominant peak in the Raman gain spectrum (blue curves with dots in Fig. 1). Because of its simplicity, this simple model is widely used to investigate ultrafast nonlinear phenomena in optical fibers. Although it explains the qualitative behavior reasonably well, this model underestimates Raman gain considerably in the frequency range below 10 THz, while overestimating it beyond 15 THz. Consequently, it does not provide a correct quantitative description of Raman-induced phenomena and leads to difficulty in comparing theory and experiments. We show in this Letter that the problem can be fixed by considering the anisotropic nature of Raman scattering and introducing an appropriate but simple form for the anisotropic part of the Raman response.

The third-order nonlinear response of silica should be described by a tensor of the form²

$$R_{ijkl}^{(3)}(\tau) = [(1-f_R)/3]\delta(\tau)(\delta_{ij}\delta_{kl} + \delta_{ik}\delta_{jl} + \delta_{il}\delta_{jk}) + f_R R_a(\tau)\delta_{ij}\delta_{kl} + (f_R/2)R_b(\tau)(\delta_{ik}\delta_{jl} + \delta_{il}\delta_{jk}), \quad (1)$$

where $i, j, k, l = x$ or y and $R_a(\tau)$ and $R_b(\tau)$ are the iso-

tropic and anisotropic parts of the Raman response, respectively. The often-used scalar form of the nonlinear response is given by $R_{xxxx}^{(3)}(\tau) = (1-f_R)\delta(\tau) + f_R[R_a(\tau) + R_b(\tau)]$.

Equation (1) indicates that the Raman gain in silica fibers consists of contributions from isotropic and anisotropic molecular responses given by $g_a(\Omega) \equiv 2\gamma f_R \text{Im}[\tilde{R}_a(\Omega)]$ and $g_b(\Omega) \equiv 2\gamma f_R \text{Im}[\tilde{R}_b(\Omega)]$, respectively, where $\gamma = n_2\omega_0/c$ is the nonlinear parameter.¹ Here, $\tilde{R}_\epsilon(\Omega)$ ($\epsilon = a, b$) is the Fourier transform of $R_\epsilon(\tau)$ defined as $\tilde{R}_\epsilon(\Omega) = \int_{-\infty}^{\infty} R_\epsilon(\tau)\exp(i\Omega\tau)d\tau$. From Eq. (1), the Raman gain for copolarized and orthogonally polarized pumps is found to be² $g_{\parallel}(\Omega) = g_a(\Omega) + g_b(\Omega)$ and $g_{\perp}(\Omega) = g_b(\Omega)/2$. Figure 2 shows the spectra of g_{\parallel} (Ref. 6) and the associated decomposed g_a and g_b (g_{\perp} is shown in Fig. 1). Although the anisotropic part provides a relatively small Raman gain for an orthogonally polarized signal, its contribution to the copolarized Raman gain dominates in the low-frequency region. Figure 2 shows clearly that it is the anisotropic response that is responsible for the shoulder around 3 THz in the copolarized Raman gain.

Physically, the isotropic Raman response stems dominantly from the symmetric stretching motion of the bridging oxygen atom in the Si—O—Si bond.³ It

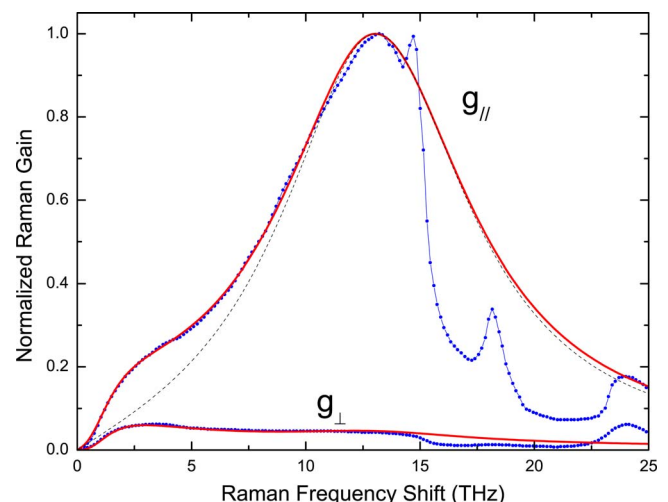


Fig. 1. (Color online) Raman gain spectra. Blue curves with dots: experimental data⁶; dashed curve, conventional Lorentzian model; red curves, our model.

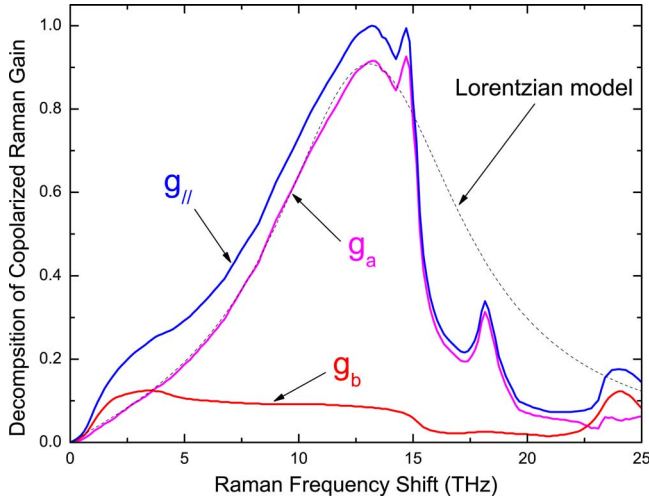


Fig. 2. (Color online) Decomposition of the copolarized Raman gain into its two parts, g_a and g_b . The dashed curve shows the fit based on the simple Lorentzian model.

turns out that this motion, and the resulting Raman gain g_a , can be described well by the widely used single-Lorentzian model. For this reason, we adopt it for the isotropic response and use $R_a(\tau) = f_a h_a(\tau)$, where $h_a(\tau)$ is given by¹⁰

$$h_a(\tau) = \tau_1(\tau_1^{-2} + \tau_2^{-2}) \exp(-\pi/\tau_2) \sin(\pi/\tau_1) \quad (2)$$

and f_a represents the fractional contribution of R_a to the total copolarized Raman response. By using the values $\tau_1 = 12.2$ fs and $\tau_2 = 32$ fs (Ref. 10) and choosing $f_a = 0.75$, we find that g_a in Fig. 2 can be fitted quite well with Eq. (2), especially in the spectral region below 14 THz. If we can find an appropriate function for the anisotropic Raman response $R_b(\tau)$, we should be able to provide an accurate description of the total nonlinear response.

Figure 2 shows that g_b , and the corresponding g_\perp in Fig. 1, exhibit a broad peak in the frequency region around 3 THz. Such a low-frequency peak is known as the Boson peak and is a universal feature of amorphous glassy substances.^{12–17} Although its physical nature is still under debate,^{12–17} the Boson peak reflects an excessive density of vibrational states. The Boson peak in g_\perp can be described by a Lorentzian function with a cubic dependence on frequency on its low-frequency side.^{12–14} We have found that the corresponding temporal response can be modeled by a simple function of the form

$$h_b(\tau) = [(2\tau_b - \tau)/\tau_b^2] \exp(-\pi/\tau_b), \quad (3)$$

where a single τ_b governs the response because of the low-frequency nature of the Boson peak.

Moreover, g_b exhibits a flat spectral plateau in the frequency range 8–15 THz that cannot be completely accounted for by Eq. (3). This plateau not only coincides with the broadband peak of g_a but also exhibits a drop-off around 15 THz, similar to g_a . These features suggest that this spectral portion of g_b shares a common physical origin with the dominant peak of g_a , probably because of the participation of other bond-bending motions or the existence of strong

intermediate-range correlations between nearby bonds.³ Based on the preceding discussion, we propose the following form for the anisotropic part of the Raman response in fused silica: $R_b(\tau) = f_b h_b(\tau) + f_c h_a(\tau)$, where f_b and f_c represent the fractional contributions of $h_b(\tau)$ and $h_a(\tau)$, respectively. In our model, the copolarized nonlinear response is given by

$$R_{xxxx}^{(3)}(\tau) = (1 - f_R) \delta(\tau) + f_R [f_a + f_c] h_a(\tau) + f_b h_b(\tau), \quad (4)$$

with $f_a + f_c + f_b = 1$. By choosing $\tau_b = 96$ fs to account for the spectral width of the Boson peak together with $f_b = 0.21$ and $f_c = 0.04$, we find in Fig. 1 that both g_\parallel and g_\perp are fitted very well by our model over the frequency range 0–15 THz.

Figures 1 and 2 show only the normalized Raman gain spectra. To obtain a realistic value of the peak Raman gain, we need to assign an appropriate value to f_R in Eq. (1). If we use $n_2 = 2.6 \times 10^{-20}$ m²/W for silica fibers,¹ the choice $f_R = 0.245$ in our model yields a peak Raman gain equal to the experimental value of $g_R = 1.2 \times 10^{-11}$ cm/W at 795.5 nm,⁴ corresponding to $g_R = 1.81 \times 10^{-11}$ cm/W at 526 nm.⁶ With this choice, not only does our model provide Raman gain accurately over the spectral range 0–15 THz, it also describes the Raman-induced changes in the nonlinear refractive index over the same frequency range well, since the two are related through the Kramers–Kronig relation.² This can be seen in Fig. 3, where we plot the nonlinear refractive index given by the real part of $\tilde{R}_{xxxx}^{(3)}(\Omega)$.

Our value of f_R is slightly higher than the experimental value of about 0.2 (Refs. 9 and 10), because our model overestimates the Raman gain in the spectral region beyond 15 THz. This causes an underestimation of the electronic contribution to nonlinear refractive index by 5% or so, as seen in Fig. 3, when the frequency shift exceeds 20 THz and where the Raman contribution is negligible. However, this underestimation does not affect the description of nonlinear effects until the pulse becomes so short that it contains only a few optical cycles. We expect our

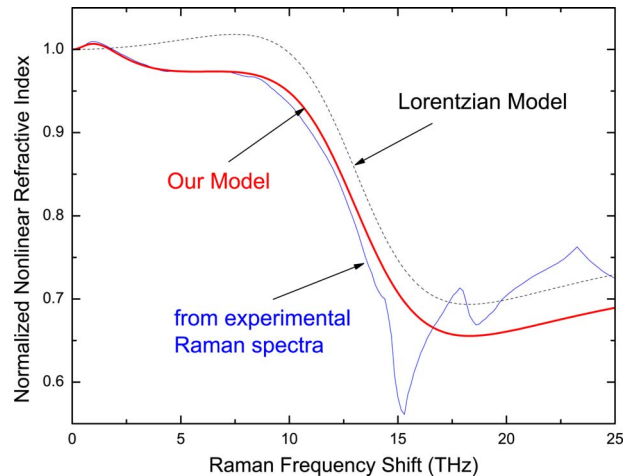


Fig. 3. (Color online) Normalized nonlinear refractive index. Blue curve, obtained from experimental Raman spectra⁶; thin dashed curve, conventional Lorentzian model; red curve, our model.

model to provide a relatively accurate description of nonlinear effects for pulses as short as 30 fs.

As a simple application of our model, we focus on the RIFS. For a linearly polarized soliton, the RIFS increases along the fiber at a rate given by¹⁸

$$\frac{d\bar{\omega}}{dz} = -\frac{E_s\Omega_0}{2\pi A_{\text{eff}}}\int_0^\infty \frac{g_{\parallel}(\Omega)(\Omega/\Omega_0)^3}{\sinh^2(\Omega/\Omega_0)}d\Omega, \quad (5)$$

where $\bar{\omega}$ is the carrier frequency of soliton, E_s is the soliton energy, $\Omega_0 = 4 \ln(1 + \sqrt{2})/(\pi T_s)$ is related to the soliton width T_s (FWHM), and A_{eff} is the effective mode area. Figure 4 shows the normalized rate of RIFS, defined as $|d\bar{\omega}/dz|A_{\text{eff}}/(g_R E_s)$. Clearly, our model provides a relatively accurate description of RIFS, and its predictions nearly coincide with that based on the experimental Raman spectra. However, the conventional single-Lorentzian model¹⁰ underestimates the RIFS rate by about 40% for pulse widths in the range of 100 to 500 fs. When pulse width decreases below 100 fs, the contribution of the broad Raman-gain peak begins to dominate, and the discrepancy between the two models decreases.

To further explore the implications of our model, we have studied propagation of a 300-fs sech pulse at 1200 nm with 960 W peak power along a 5 m long microstructured fiber numerically by solving the generalized nonlinear Schrödinger equation.¹ The fiber with a 2.5 μm core diameter is assumed to have a large air-filling fraction, so its dispersion can be modeled as a glass rod surrounded by air. The inset of Fig. 4 shows the output spectra. Because of fiber dispersion, the input pulse splits into two parts, one of which forms a soliton whose width changes from about 60 to 100 fs along the fiber, resulting in a net

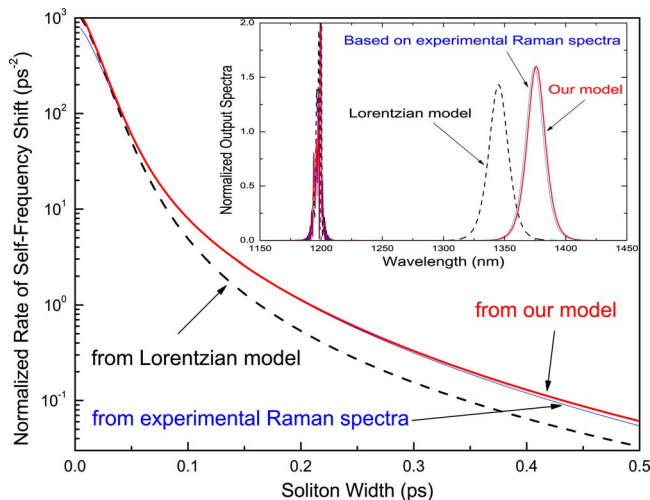


Fig. 4. (Color online) RIFS rate versus soliton width T_s for our model (red curve) and conventional model (dashed curve). The blue curve is based on the experimental Raman spectrum. Inset, output spectra obtained numerically for a 300 fs pulse, assumed to maintain its linear polarization.

RIFS of 175 nm. Our proposed model shows excellent agreement with the one obtained numerically using the experimental Raman spectrum. However, the conventional model based on Eq. (2) underestimates the RIFS by about 20%.

In conclusion, we show that the conventional single-Lorentzian model does not provide an accurate quantitative description of the Raman response. The reason is found to be related to the anisotropic part of the Raman response that is ignored by this often-used model. Based on the notion of the Boson peak, we introduce a simple function to account for this anisotropic part and show that the new model fits quite well both the Raman gain and the Raman-induced changes in the nonlinear refractive index over a frequency range 0–15 THz. We expect that our model would provide a much more accurate description of the propagation of ultrashort pulses. Our model can also be used to describe quantitatively various Raman-related vectorial nonlinear phenomena.

This work is supported by the National Science Foundation under grant ECS-0320816.

References

1. G. P. Agrawal, *Nonlinear Fiber Optics*, 3rd ed. (Academic, 2001), Chap. 2.
2. R. W. Hellwarth, *Prog. Quantum Electron.* **5**, 1 (1977).
3. F. L. Galeener, A. J. Leadbetter, and M. W. Stringfello, *Phys. Rev. B* **27**, 1052 (1983); and references therein.
4. D. J. Dougherty, F. X. Kärnter, H. A. Haus, and E. P. Ippen, *Opt. Lett.* **20**, 31 (1995).
5. A. K. Atieh, P. Myslinski, J. Chrostowski, and P. Galko, *J. Lightwave Technol.* **17**, 216 (1999).
6. R. H. Stolen, in *Raman Amplifiers for Telecommunications I*, M. N. Islam, ed. (Springer, 2003). Raman spectra are provided by R. H. Stolen.
7. F. A. Oguama, H. Garcia, and A. M. Johnson, *J. Opt. Soc. Am. B* **22**, 426 (2005); and references therein.
8. I. Mandelbaum, M. Bolshtyansky, T. F. Heinz, and A. R. H. Walker, *J. Opt. Soc. Am. B* **23**, 621 (2006).
9. R. H. Stolen, J. P. Gordon, W. J. Tomlinson, and H. A. Haus, *J. Opt. Soc. Am. B* **6**, 1159 (1989).
10. K. J. Blow and D. Wood, *IEEE J. Quantum Electron.* **25**, 2665 (1989).
11. D. Hollenbeck and C. D. Cantrell, *J. Opt. Soc. Am. B* **19**, 2886 (2002).
12. V. K. Malinovsky and A. P. Sokolov, *Solid State Commun.* **57**, 757 (1986).
13. V. K. Malinovsky and A. P. Sokolov, *Glass Phys. Chem.* **22**, 152 (1996).
14. C. McIntosh, J. Toulouse, and P. Tick, *J. Non-Cryst. Solids* **222**, 335 (1997).
15. E. Courtens, M. Foret, B. Hehlen, and R. Vacher, *Solid State Commun.* **117**, 187 (2001); and references therein.
16. V. L. Gurevich, D. A. Parshin, and H. R. Schober, *Phys. Rev. B* **67**, 094203 (2003); and references therein.
17. N. Shimodaira, K. Saito, N. Hiramitsu, S. Matsushita, and A. J. Ikushima, *Phys. Rev. B* **71**, 024209 (2005).
18. J. P. Gordon, *Opt. Lett.* **11**, 662 (1986).